

Modeling molecular motors

Frank Jülicher,* Armand Ajdari,† and Jacques Prost‡

Physicochimie Curie, U.M.R. 168, Institut Curie, 26 rue d'Ulm, F-75231 Paris Cedex 05, France and Laboratoire de Physico-Chimie Théorique, U.R.A. 1382, ESPCI, 10 rue Vauquelin, F-75231 Paris Cedex 05, France

The authors present general considerations and simple models for the operation of isothermal motors at small scales, in asymmetric environments. Their work is inspired by recent observations on the behavior of molecular motors in the biological realm, where chemical energy is converted into mechanical energy. A generic Onsager-like description of the linear (close to equilibrium) regime is presented, which exhibits structural differences from the usual Carnot engines. Turning to more explicit models for a single motor, the authors show the importance of the time scales involved and of the spatial dependence of the motor's chemical activity. Considering the situation in which a large collection of such motors operates together. The authors exhibit new features among which are dynamical phase transitions formally similar to paramagnetic-ferromagnetic and liquid-vapor transitions. [S0034-6861(97)00304-8]

CONTENTS

I. Introduction	1269
II. Motion and Efficiency Close to Thermal Equilibrium	1271
III. A Two-State Model for a Single Motor	1272
IV. Collective Effects	1276
V. Concluding Remarks	1280
Acknowledgments	1280
References	1281

I. INTRODUCTION

Modern biology has shown that an important number of biological processes are governed by the action of molecular complexes reminiscent in some way of macroscopic machines (Kreis and Vale, 1993; Alberts *et al.*, 1994). For instance, the words “channels” and “pumps” are commonly used to describe protein aggregates promoting, respectively, passive and active transport of ions and molecules across biological membranes, whereas the word “motor” is used for proteins or protein complexes that transduce at a molecular scale chemical energy into mechanical work. Both rotatory and translational motors are known to exist. In this colloquium article, we focus our attention on translational (or “linear”) molecular motors. We do not give a full review of their modeling, but rather present a generic and simple description, which allows one to extract the main features of the physics involved, deliberately avoiding the biological complexity.

Extensive studies over the last twenty years have shown that a significant part of the eukaryotic cellular traffic relies on “motor” proteins that move in a deter-

ministic way along filaments similar in function to railway tracks or freeways (see Fig. 1). Three different families of motor proteins have been identified: kinesins and dyneins move along tubulin filaments, myosins move along actin filaments. For what follows, we need only to know that the filaments are periodic and fairly rigid structures with a period of the order of 10 nm. They are moreover polar, so that one can define a “plus” and a “minus” extremity. A given motor always moves in the same direction. Myosin moves along actin filaments towards their plus extremity, and kinesins and dyneins move along tubulin filaments towards their plus and minus extremities respectively. From the complex structure of the motors we need to remember the existence of two “heads” interacting with filaments of a size comparable to the filament period (single-headed motor proteins can also be engineered, and dyneins may in some cases have three heads), as well as the existence of a tail several tens of nanometers long, able to attach to vesicles or assemble in bundles as in muscle fibers. Motor molecules play a key role not only in muscular contraction but also in cell division, cellular traffic, material transport along the axons of nerve cells, etc. (Alberts *et al.*, 1994).

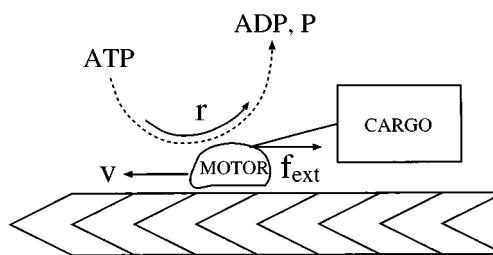


FIG. 1. Cartoon of a motor protein moving with velocity v along a periodic and polar track filament. As it carries some cargo along its way, it moves against an external force f_{ext} and consumes r ATP molecules per unit time, which are hydrolyzed to ADP and phosphate (P).

*Electronic address: frank.julicher@curie.fr

†Electronic address: armand@turner.pct.espci.fr

‡Electronic address: jacques.prost@curie.fr

The experimental work on muscles, dating back to the early ages of the microscope, was *de facto*, looking at macroscopic manifestations of the function of molecular motors. Excellent early reviews on the modeling of muscle contraction can be found in A. F. Huxley (1957) and Hill (1974). A key point in these theories lies in the existence of several states of a motor, within each of which the system reaches local thermodynamic equilibrium on time scales small compared to the exchange rates between these states. Local thermodynamic equilibrium is meaningful because of the following comparison of orders of magnitude: from the transient response of muscles it was known that the fastest characteristic times of the motors were in the range of milliseconds. Thermal equilibrium occurs on length scales of 10 nm after tens to at most hundreds of nanoseconds. The states of the proteins during muscular contraction therefore had to be in local thermal equilibrium. Up to five and even six different states could be involved¹ (Lynn and Taylor, 1971; Hill, 1974). Clearly identified were the need for asymmetry (i.e., polarity of the motor/filament interaction), the importance of chemical energy consumption and, in a more subtle way, the relevance of the fact that the periodicities of motors and filament are incommensurate. All of these points will be illustrated in the following. In the earliest theoretical description, the asymmetry of the system was introduced via asymmetric transition rates (A. F. Huxley, 1954). Specific conformational changes were also discussed (H. E. Huxley, 1969; A. F. Huxley and Simmons, 1971).

The recent revival of interest in the modeling of molecular motors stems from the appearance of a new generation of experiments. Both the filaments and the motor proteins can be purified to such an extent that clean reproducible experiments can be performed *in vitro*. These experiments can be divided in two classes: (i) the optical monitoring of motion of single filaments propelled by many motors, which are absorbed on a flat substrate (Kron and Spudich, 1986; Harada *et al.*, 1987; Spudich, 1990; Ishijima *et al.*, 1991; Winkelmann *et al.*, 1995); or (ii) the observation of motion of single motors along filaments. The second type of experiment is achieved by coating a micron-sized silica bead with a small number of motors and observing the bead motion along a single filament induced by the interaction of one of the motors with the filament (Svoboda *et al.*, 1993; Hunt *et al.*, 1994; Svoboda and Block, 1994). Alternatively, the motion of filaments interacting with single motors can be monitored (Ishijima *et al.*, 1991; Finer *et al.*, 1994). Details as refined as the elementary “stepping” events can be identified. The first class of experiments (called motility assays) typically involves a large number of motors interacting with a filament. Such motor collections are fairly similar to the arrangement of motors in muscle fibers. The second class of experiments, more relevant to our understanding of eucariotic intracellular transport, raises the question of the inter-

ference of fluctuations and Brownian motion with the directed motion that is characteristic of these motors.

From a theoretical point of view, molecular motors are microscopic objects that unidirectionally move along one-dimensional periodic structures. The problem of explaining this unidirectionality belongs to a larger class of such problems involving rectifying processes at small scale. A simple model of such a process is a generalization of Feynman’s famous “thermal ratchet” (Feynman *et al.*, 1966). Büttiker (1987) and Landauer (1988) showed that a periodic distribution of temperatures with the proper asymmetry was sufficient to induce macroscopic motion of a particle in a periodic potential via a rectification mechanism of the random Brownian forces. As already discussed, any temperature inhomogeneity at the scale of a few tens of nanometers decays on time scales of microseconds, so that even though the developed concept is very attractive it cannot be retained for describing motors at the nanometer scale. Note that periodic temperature gradients in the micron range can be produced: it would be quite interesting to design experiments able to check the predictions of Büttiker and Landauer.

Various isothermal rectifying processes have been discussed. For instance in the context of biophysics they were invoked both for the function of ion pumps (Astumian *et al.*, 1987) and for the translocation of proteins (Simon *et al.*, 1992). Periodic isothermal ratchets have been discussed from different perspectives (Doering, 1995; Astumian, 1997). We can distinguish three different approaches.

(i) *Fluctuating forces*: a pointlike particle is placed in a periodic, asymmetric potential $W(x)$ and is submitted to a fluctuating force that does not satisfy a fluctuation-dissipation theorem. Typically the particle motion is described by the Langevin equation

$$\xi \frac{dx}{dt} = -\partial_x W(x) + F(t), \quad (1)$$

where ξ is a constant friction coefficient, x the position of the particle, and $W(x)$ the potential energy it experiences. The fluctuating force $F(t)$ has zero averaged value, $\langle F(t) \rangle = 0$, but has richer correlation functions than a simple Gaussian white noise. These correlations of the fluctuating forces reflect the energy source: their structure depends for example on the complexity of an underlying chemical process. As soon as the fluctuation-dissipation theorem is broken, a rectified motion sets in with a direction that depends in a subtle manner on the details of the statistics (Büttiker, 1987; Landauer, 1988; Magnasco, 1993; Doering *et al.*, 1994; Magnasco, 1994; Millonas and Dykman, 1994; Chialvo and Millonas, 1995; Luczka *et al.*, 1995; Mielke, 1995a, 1995b; Millonas, 1995; Bartussek *et al.*, 1996). A time-dependent external force leads to similar results (Magnasco, 1993; Ajdari *et al.*, 1994; Bartussek *et al.*, 1994). In principle, inertial terms could be added in Eq. (1). The motion of a massive particle subject to a fluctuating force is a beautiful theoretical problem (Hondou and Sawada, 1995; Jung *et al.*, 1996). We shall not go into this subject here:

¹Note that a continuum of states cannot be ruled out *a priori*.

indeed, the characteristic crossover time between underdamped and overdamped behavior is of the order of a few picoseconds on the 10-nm scale.

(ii) *Fluctuating potentials*: A pointlike particle is placed in a periodic, asymmetric potential with a value that depends on time:

$$\xi \frac{dx}{dt} = -\partial_x W(x,t) + f(t). \quad (2)$$

x , ξ , and W keep the same meaning as in Eq. (1) but the potential W depends explicitly on time, and the random forces $f(t)$ are Gaussian white noise which obeys a fluctuation-dissipation theorem:

$$\langle f(t) \rangle = 0, \quad \langle f(t)f(t') \rangle = 2\xi T \delta(t-t'). \quad (3)$$

The energy source is now implicit in the time dependence of the potential W . Most works have considered the case in which $W(x,t) = A(t)V(x)$ (Ajdari, 1992; Ajdari and Prost, 1992; Astumian and Bier, 1994; Doering, 1995). If $A(t)$ is a random variable which can adopt two different values and if the distribution of residence times at each value is given by a Poisson distribution, Eq. (2) corresponds to the motion of a particle fluctuating between different states for which the transition rates between states are constant.

(iii) *Particle fluctuating between states*: the notion of well-defined states, introduced earlier in the discussion of muscles, is used (Chauwin *et al.*, 1994; Peskin *et al.*, 1994; Prost *et al.*, 1994; Zhou and Chen, 1996; Harms and Lipowsky, 1997). In each of the states, the ‘‘particle’’ experiences a classical Langevin equation:

$$\xi_i \frac{dx}{dt} = -\partial_x W_i(x) + f_i(t). \quad (4)$$

Here, the index i refers to the considered state, $i = 1 \dots N$, and $f_i(t)$ satisfies a fluctuation-dissipation theorem:

$$\langle f_i(t) \rangle = 0, \quad \langle f_i(t)f_j(t') \rangle = 2\xi_i T \delta(t-t') \delta_{ij}. \quad (5)$$

The dynamics of transitions between the states have to be added independently, which is most conveniently done in a Fokker-Planck formalism, as will be discussed in Sec. III. Rectification is obtained only to the extent that at least one of the transitions does not satisfy detailed balance. Although approaches (i) to (iii) may differ in the details of the rectification process, they share in common their main features.

Aiming at a more realistic description on the molecular level, several authors have added internal variables (which become necessary if the time required to achieve, for instance, a conformational change is not small compared to other time scales), in particular in order to quantify the significance of correlations between the two heads of the motors (Ajdari, 1994; Peskin and Oster, 1995; Derényi and Vicsek, 1996; Duke and Leibler, 1996). Such models often aim at describing more closely specific features of particular biological motors, such as the two-head walk of kinesin or the power stroke of myosin.

In the next sections, and in the spirit of a colloquium

article, we focus on a simple description in which we keep only two different states. This approach follows the basic idea of the Ising model for phase transitions: the aim is not to describe molecular details but to extract generic features of motion generation and to extend the modeling to the case of many motors. The generic properties we extract can be used as guides not only to the understanding of molecular motors but also to the conception of new particle separation devices.

In Sec. II, following the early analysis of Kedem and Caplan (1965), we illustrate the originality of isothermal motors by analyzing their behavior close to thermal equilibrium using a simple linear-response theory. In particular, we calculate the efficiency of these motors and show how they differ from Carnot engines. The results presented in this section are completely independent of any underlying microscopic mechanism. In real life, molecular motors work in fact far from equilibrium: to go further, and in particular to be able to discuss non-linear regimes, one needs to construct more specific models. In Sec. III, we introduce the two-state model: we choose it because it is simple enough to be tractable and generic enough to give physical insight into many physical realizations. We show the importance both of the time scales involved and of the spatial dependence of chemical activity within the motor. In Sec. IV, we consider the situation in which a large number of motors operate together and concentrate on the qualitatively new features that emerge from the many-motor problem: We show the existence of a dynamical phase transition formally similar to the liquid-vapor transition. One natural consequence of this phase transition is the possibility of spontaneous oscillations whenever elastic elements are added in series to the motor collection. This feature could be relevant to the understanding of the oscillations of insect flight muscles such as those of wasps and bees (Pringle, 1977; Yasuda *et al.*, 1996). In our concluding remarks we summarize the main ideas and discuss possible technological applications of the concepts discussed here.

II. MOTION AND EFFICIENCY CLOSE TO THERMAL EQUILIBRIUM

As explained above, molecular motors are isothermal, which implies that internal states can be defined that are locally in equilibrium at a constant temperature T . The action of the motor is induced by generalized forces, which for the motor/filament system may be identified as the mechanical force f_{ext} applied to the motor, and the chemical potential difference $\Delta\mu$, which measures the free-energy change per consumed ‘‘fuel’’ molecule. The force f_{ext} describes external forces, for example of optical tweezers, microneedles, or the viscous load of an object that is carried. f_{ext} could also include viscous friction forces between the motor and the surrounding solvent if the latter is considered as ‘‘external.’’ The chemical potential difference $\Delta\mu$ is for the process of the hydrolysis of adenosinetriphosphate (ATP) to adenosinediphosphate (ADP) and phosphate (P), $\text{ATP} \rightleftharpoons \text{ADP} + \text{P}$, given

by $\Delta\mu = \mu_{\text{ATP}} - \mu_{\text{ADP}} - \mu_{\text{P}}$. At chemical equilibrium $\Delta\mu = 0$, whereas it is positive when ATP is in excess and negative when ADP is in excess. The action of these generalized forces leads to motion and fuel consumption, characterized by generalized “currents”—the average velocity v and the average rate of consumption of fuel molecules r (i.e., the average number of ATP molecules hydrolyzed per unit time, per motor).

The dependencies $v(f_{\text{ext}}, \Delta\mu)$ and $r(f_{\text{ext}}, \Delta\mu)$ of velocity and fuel consumption as functions of forces are in general nonlinear. Molecular motors mostly operate far from equilibrium ($\Delta\mu \approx 10k_B T$), where these nonlinearities are important. However, it is instructive first to explore the linear regime ($\Delta\mu \ll k_B T$). In this regime, a linear-response theory holds (Hill, 1974; Jülicher *et al.*, 1997), which allows us to write

$$\begin{aligned} v &= \lambda_{11}f_{\text{ext}} + \lambda_{12}\Delta\mu, \\ r &= \lambda_{21}f_{\text{ext}} + \lambda_{22}\Delta\mu. \end{aligned} \quad (6)$$

Here, we have introduced a mobility coefficient λ_{11} and the mechano-chemical coupling coefficients λ_{12} and λ_{21} . The latter are nonzero only if the filaments are polar. λ_{22} is a generalized mobility relating ATP consumption and chemical potential difference. On general grounds, an Onsager relation holds: $\lambda_{12} = \lambda_{21}$ (Hill, 1974). The stability of the system requires $\lambda_{ii} > 0$ and $\lambda_{11}\lambda_{22} - \lambda_{12}\lambda_{21} > 0$. This insures that the dissipation rate Π is positive:

$$\Pi = f_{\text{ext}}v + r\Delta\mu > 0. \quad (7)$$

Whenever $f_{\text{ext}}v < 0$, work is performed by the motor; whenever $r\Delta\mu < 0$, chemical energy is generated. Thus a given motor/filament system can work in any of eight different regimes (see Fig. 2). Four of them are essentially passive,² whereas the other four are more interesting: uses ATP and ADP in one of the following ways:

(A) $r\Delta\mu > 0, f_{\text{ext}}v < 0$: the motor uses the hydrolysis of ATP in excess to generate work,

(B) $r\Delta\mu < 0, f_{\text{ext}}v > 0$: the system produces ATP already in excess from mechanical input,

(C) $r\Delta\mu > 0, f_{\text{ext}}v < 0$: the motor uses ADP in excess to generate work,

(D) $r\Delta\mu < 0, f_{\text{ext}}v > 0$: the system produces ADP already in excess from mechanical input.

Linear-response theory tells us that a sign change of $\Delta\mu$ leads to a velocity reversal of the motor. This phenomenon may be out of reach for the currently known molecular motors, which operate in general in the nonlinear extension of regime A far from equilibrium. However, this velocity reversal is conceptually interesting

²If both $f_{\text{ext}}v$ and $r\Delta\mu$ are positive, there is no energy output from the system. Instead, all work performed at the system is simply dissipated in the thermal bath. This is what we call a purely passive system. The case for which both $f_{\text{ext}}v$ and $r\Delta\mu$ are negative would imply that the system performs both mechanical and chemical work, taking the energy from a single heat bath. This case is forbidden by the second law of thermodynamics, which requires $\Pi > 0$.

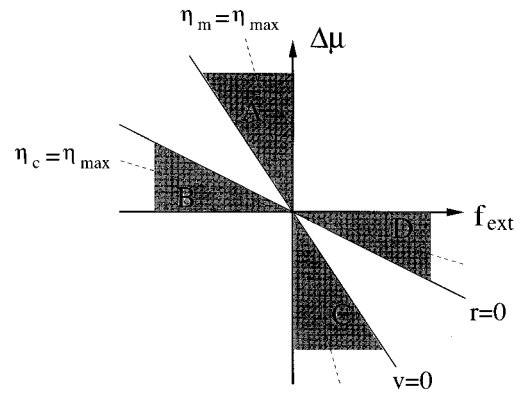


FIG. 2. Operation diagram for an isothermal chemical motor in the linear regime as a function of externally applied force f_{ext} and chemical force $\Delta\mu$. In regimes A and C, the motor transforms chemical energy into work, while in regimes B and D it generates chemical energy from mechanical input. Lines of maximal mechanical efficiency η_m and chemical efficiency η_c are indicated.

since it allows direction reversal without any need for changing the microscopic mechanism.

Efficiencies are also worth consideration. In regimes A and C one can define the efficiency as for any macroscopic motor,

$$\eta_m = -\frac{f_{\text{ext}}v}{r\Delta\mu}, \quad (8)$$

that is, by the ratio of mechanical work performed to chemical energy consumed. For regimes B and D, the quantity of interest is the chemical efficiency

$$\eta_c = -\frac{r\Delta\mu}{f_{\text{ext}}v}, \quad (9)$$

which is the inverse of the mechanical efficiency. Clearly the efficiencies vanish along the boundaries of the corresponding domains (where either v , f_{ext} , r , or $\Delta\mu$ vanish), and they have a constant maximal value $\eta_{\text{max}} = (1 - \sqrt{1 - \Lambda})^2 / \Lambda$ with $\Lambda = \lambda_{12}^2 / (\lambda_{11}\lambda_{22})$ along straight lines merging at the origin. Thus thermal equilibrium ($\Delta\mu = 0, f_{\text{ext}} = 0$) represents a singular limit: At this point the efficiencies given by Eqs. (8) and (9) are not defined. In the limit where equilibrium is approached starting from one of the regimes A–D, a finite efficiency is reached. Note also that the often expressed statement that efficiency is maximum around “stall force” (i.e., the force for which $v = 0$ for a given value of $\Delta\mu$) is wrong: at stall force the efficiency vanishes. This is an important difference from Carnot engines, which have maximal efficiency at stall conditions when the Carnot engine operates reversibly.

III. A TWO-STATE MODEL FOR A SINGLE MOTOR

We shall now discuss a concrete model for force generation and motion of linear molecular motors. We restrict our analysis to a two-state model (Peskin *et al.*,

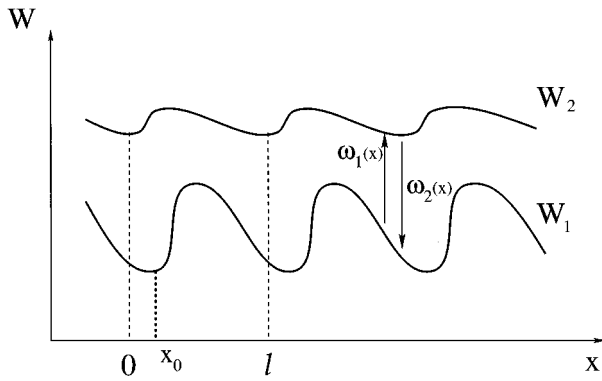


FIG. 3. Schematic picture of the two l -periodic asymmetric potentials. Although the two potentials are flat on a larger scale, motion is expected when the ratio of transition rates ω_1/ω_2 is driven away from its equilibrium value given by Eq. (15).

1994; Prost *et al.*, 1994), in which the fuel consumption triggers a conformational change between two states 1 and 2. Transitions between these states are described by standard chemical kinetics. For each of the states, a position-dependent one-dimensional potential can be defined in the following way: The motor is allowed to find its equilibrium position close to the filament with the constraint that the x coordinate of the center of mass is given. The free energy of the motor in state i confined at point x defines the potential $W_i(x)$. This definition implies that the symmetry of the filament is reflected in the symmetry of the potentials: $W_i(x)$ is both periodic and asymmetric. Note that this potential is defined for any x , irrespective of the range of interactions involved. The variations of this potential can in principle be estimated by measuring the force required to maintain the particle at the prescribed position x . An experiment along these lines suggests that the distance between minimum and maximum is of the order of 3 nm for actin/myosin (Nishizaka *et al.*, 1995), but in general we do not know the potential shape.

In order to develop a stochastic description of the dynamics, we introduce the probability density $P_i(x,t)$ for the motor to be at position x at time t in state i . This periodic system with period l is shown schematically in Fig. 3. The evolution of the system can be described by two Fokker-Planck equations with source terms:

$$\partial_t P_1 + \partial_x J_1 = -\omega_1(x)P_1 + \omega_2(x)P_2, \quad (10)$$

$$\partial_t P_2 + \partial_x J_2 = \omega_1(x)P_1 - \omega_2(x)P_2, \quad (11)$$

where the currents result from diffusion, interaction with the filament, and the action of a possible external force f_{ext} :

$$J_i = \mu_i [-k_B T \partial_x P_i - P_i \partial_x W_i + P_i f_{\text{ext}}]. \quad (12)$$

The source terms are determined by the rates $\omega_i(x)$ at which the motor switches from one state to the other. The functions $\omega_i(x)$ again have the symmetry properties of the filament.

The set of Eqs. (10)–(12) can be used not only to il-

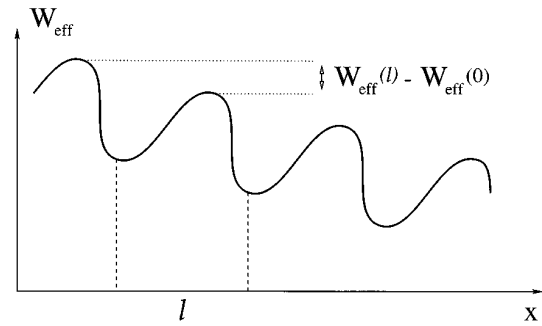


FIG. 4. Schematic picture of the effective potential $W_{\text{eff}}(x)$ acting on the particle if the transition rates between the two states do not obey detailed balance.

lustrate the motion of molecular motors but also to show explicitly in terms of an effective one-dimensional equation how this motion and force generation emerge. This effective description is obtained by evaluating the steady-state particle current $J = J_1(x) + J_2(x)$ for l -periodic $P_i(x)$. Introducing $P = P_1 + P_2$ and $\lambda(x) = P_1(x)/P(x)$, it takes the form

$$J = \mu_{\text{eff}} [-k_B T \partial_x P - P \partial_x W_{\text{eff}} + P f_{\text{ext}}] \quad (13)$$

with an effective mobility given by $\mu_{\text{eff}} = \mu_1 \lambda + \mu_2 (1 - \lambda)$ and an effective potential that reads

$$W_{\text{eff}}(x') - W_{\text{eff}}(0) = \int_0^{x'} dx \frac{\mu_1 \lambda \partial_x W_1 + \mu_2 (1 - \lambda) \partial_x W_2}{\mu_1 \lambda + \mu_2 (1 - \lambda)} + k_B T [\ln(\mu_{\text{eff}})]_0^{x'}. \quad (14)$$

One can show that, with periodic boundary conditions, $\lambda(x)$ has the potential symmetry. So if the potential is symmetric, the integrand in Eq. (14) is antisymmetric and the effective potential is periodic: $W_{\text{eff}}(nl) = W_{\text{eff}}(0)$ for integer n . It is thus flat on large scales and cannot generate motion.

For asymmetric potentials, the effective potential generically has a nonzero average slope $[W_{\text{eff}}(l) - W_{\text{eff}}(0)]/l$ on large scales (see Fig. 4), although W_1 and W_2 are flat on large scales (see Fig. 3). This average slope corresponds to an average force that the motor develops, able to generate motion against weaker external forces f_{ext} .

However, this average force exists (i.e., the system operates as a motor) only if the system consumes chemical energy. If no energy is provided to the system, detailed balance has to be satisfied:

$$\omega_1(x) = \omega_2(x) \exp \left[\frac{W_1(x) - W_2(x)}{k_B T} \right]. \quad (15)$$

As a consequence $\lambda = (1 + \exp[(W_1(x) - W_2(x))/k_B T])^{-1}$ and W_{eff} is the l -periodic free energy of the motor, which is obviously flat on large scales. Thus breaking detailed balance is also a clear requirement for spontaneous motion.

As already discussed, in biological systems detailed balance is broken most of the time by ATP hydrolysis. Let us assume that an hydrolysis event triggers, say, the

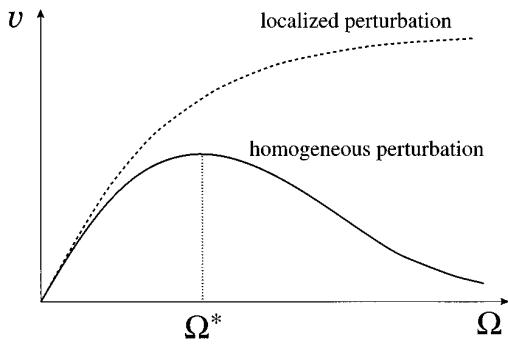


FIG. 5. Schematic diagram of the spontaneous average velocity v (for zero external force $f_{\text{ext}}=0$) of the particle as a function of Ω , which measures the departure from equilibrium and is related to the fuel concentration [see Eq. (17)].

change of the motor from state 1 to state 2 (the other choice would give similar results). Then standard chemical kinetics allows us to write

$$\begin{aligned}\omega_1(x) &= (\alpha(x)e^{\mu_{\text{ATP}}/k_B T} + \omega(x))e^{W_1(x)/k_B T}, \\ \omega_2(x) &= (\alpha(x)e^{(\mu_{\text{ADP}} + \mu_P)/k_B T} + \omega(x))e^{W_2(x)/k_B T}.\end{aligned}\quad (16)$$

The $\alpha(x)$ term corresponds to the transitions induced by the chemical reaction, and the $\omega(x)$ represents the thermally excited ones. Note that α and ω have to be l -periodic functions but are otherwise *a priori* not specified. Let us construct a quantity measuring the local deviation from detailed balance:

$$\Omega(x) = \omega_1(x) - \omega_2(x) \exp\left[\frac{W_1(x) - W_2(x)}{k_B T}\right].\quad (17)$$

Using Eq. (16), one finds

$$\Omega(x) = \alpha(x) \exp\left[\frac{W_1(x) + \mu_{\text{ATP}}}{k_B T}\right] (1 - e^{-\Delta\mu/k_B T}),\quad (18)$$

in which we have used our earlier definition of $\Delta\mu$. For practical purposes, we write $\Omega(x) = \Omega\theta(x)$, where the perturbation amplitude Ω measures the distance to equilibrium and $\int_0^l \theta(x) dx$ is normalized to one. For $\Delta\mu \rightarrow 0$, Ω vanishes linearly with $\Delta\mu$ in accordance with our choice of generalized forces. For $\Delta\mu \gg k_B T$ it is essentially proportional to the ATP concentration (which is the relevant case for biological motors).

More generally the transition rates may be perturbed by any means, for example in the case of artificially constructed systems by photon fluxes, which could induce state changes provided an appropriate frequency range were chosen. In this case, Ω and $\theta(x)$ are still a good measure of both the intensity and the spatial dependence of a departure from the equilibrium transition rates.

As a result of broken detailed balance, the motor begins to move on average and can work mechanically against a load as described by Eqs. (13) and (14). Its average velocity v is determined by $J = v \int_0^l dx P(x)/l$. However, to get explicit expressions for the velocity and the efficiency of the process, one needs to calculate $\lambda(x)$

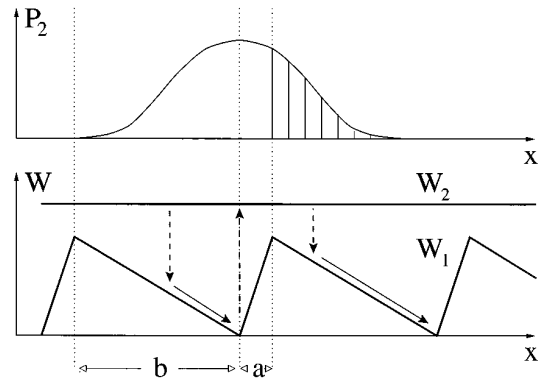


FIG. 6. Motion generation for $W_2 = \text{const}$ and $f_{\text{ext}} = 0$: A particle trapped in state 1 is excited to state 2, where it diffuses freely. It returns to state 1 after a typical lifetime ω_2^{-1} when it has a Gaussian probability distribution P_2 . With a probability proportional to the hatched area of the Gaussian distribution, it arrives at the next minimum of W_1 provided it has sufficient time in state 1 to slide to that minimum.

and thus solve Eqs. (10)–(12). It is then necessary to specify the potential shapes in order to get specific results. For $\Delta\mu/(k_B T) \ll 1$ and $f_{\text{ext}}l/(k_B T) \ll 1$, one recovers the linear regime described in Sec. II, and it is possible to verify analytically the Onsager symmetry relations (Jülicher *et al.*, 1997). An analytical treatment is also possible beyond the linear regime for piecewise linear potentials and a piecewise constant perturbation $\theta(x)$ if the “deexcitation” rate ω_2 is taken constant and if at the same time $W_2 - W_1 \gg k_B T$, which permits neglect of thermally excited transitions from conformation 1 to 2. In this “far from equilibrium” situation, Eqs. (10)–(12) can be solved using standard linear algebra (Prost *et al.*, 1994). In more general situations one should solve these equations numerically.

Two interesting limits can be identified: a homogeneous perturbation $\theta(x) = 1/l$, or a perturbation “localized” in the vicinity of the minima of W_1 , $\theta(x) = \sum_n \delta(x - x_0 + nl)$. The latter case corresponds to the notion of “active sites” in biology: it tells us that the (ATP-assisted) transition from state 1 to 2 is basically impossible, except when the protein is at a specific location along the filament. Independent of any detailed calculation, it is easy to show that the behavior of the spontaneous velocity v ($f_{\text{ext}} = 0$) as a function of the excitation rate Ω differs fundamentally in these two cases (Fig. 5).

In the first case of a homogeneous perturbation, a well-defined velocity maximum occurs at a given value of Ω . Indeed, for low excitation rates, the system is close to thermodynamic equilibrium and v grows linearly with Ω starting from zero at $\Omega = 0$ in agreement with linear-response theory. At very large Ω , only state 2 is populated, which restores a Boltzmann distribution in this state, so that in the absence of an external force the velocity vanishes as $1/\Omega^3$. The maximum velocity is obtained when two pairs of characteristic times are matched. This can be understood in the case of a constant potential W_2 (Fig. 6): suppose the particle starts

from an energy minimum of the ground state 1 and gets excited to state 2. In this state it will undergo a diffusion process, which will lead after a time t to a Gaussian probability distribution with halfwidth $(2k_B T \mu_2 t)^{1/2}$. After a typical lifetime $\tau_2 = \omega_2^{-1}$, the particle will return to the ground state. Depending on whether this transition takes place on the right or the left of the maximum of $W_1(x)$, the process will contribute to net motion (to the right) or not, as shown in Fig. 6. We want the number of favorable events contributing to the net motion to be as large as possible: A short lifetime τ_2 would yield a small contribution to motion but letting the diffusive stage last too long would allow the particle to jump to the left with an appreciable probability too. So, in scaling form, optimal conditions read $\tau_2 \approx a^2/k_B T \mu_2$ (for the definition of the length a , see Fig. 6). Now we want the particle that moved over the barrier to have sufficient time in state 1 to drift down the potential slope to reach the next minimum. Since waiting there would lead to a loss of time, the second time matching for optimization is $\tau_1 = \omega_1^{-1} = \Omega^{-1} \approx b^2/(\mu_1 W_1)$. This determines the value Ω^* at which the maximum velocity is reached in Fig. 5.

In the second case of highly localized excitations, there is no maximum in the $v(\Omega)$ curve. Indeed, while the previously mentioned time matching in state 2 is still needed, particles will now always drift downhill to the energy minimum of state 1 before being reexcited to state 2. The less time spent in the minimum, the faster the cycle and the larger the velocity. Thus the maximum is pushed towards $\Omega = \infty$.

Note that in both cases a diffusive step is needed. This is due to the fact that in the situation of Fig. 3, the particle has to escape from a valley by diffusion in either state 1 or state 2. Thus the case considered in Fig. 6, where one of the potentials is flat, allows for the fastest escape. If the mobilities μ_1 and μ_2 are comparable, the velocity scale is consequently limited by the “slow” diffusive step, so that a typical value is $v_{\text{typical}} = (\mu_2 \omega_2/k_B T)^{1/2}$, which under optimal conditions is equivalent to $v_{\text{typical}} \approx a/\tau_2 \approx \mu_2 k_B T/a$. Using the approximations described above to get analytical results, one can show that the maximum velocity is about twice as large for a localized perturbation as for a homogeneous one, everything else being kept alike. Indeed, not every drift event down towards the potential minimum is efficient in the case of homogeneous perturbations, where particles may be excited before actually reaching the minimum, whereas they are all efficient in the other case.

Note also that we have discussed here two extremes: a homogeneous perturbation $\theta(x) = 1/l$ and a perturbation localized to a point $\theta(x) = \delta(x \bmod l)$, whereas in general one expects a smoother function of x . In this intermediate case, a maximum of the velocity still exists for finite Ω , but the velocity does not vanish for large Ω . Experimental curves for motor proteins show no evidence for a maximum when the velocity is plotted as a function of the ATP concentration. This observation supports the idea of active sites.

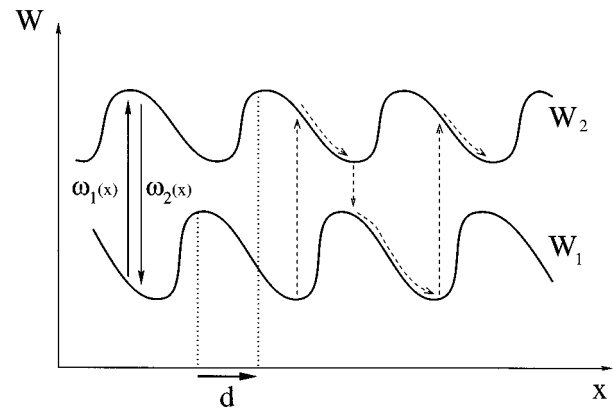


FIG. 7. “Shifted” potentials: if the “shift” d between the extrema of the two potentials is large enough, the particle can drift without having to overcome energy barriers by diffusion, a scenario more efficient than that shown in Fig. 3.

It may seem naive to compare the results of a calculation based on point particles with the behavior of a system involving complex objects such as proteins whose size is comparable to the period of the track filament. The conformation changes necessarily take time and may result in spatially rearranged binding sites. This may involve a displacement of the center of mass of the motor along the filament, contributing to the net motion and would correspond for instance to the idea of power strokes (H. E. Huxley, 1969; A. F. Huxley and Simmons, 1971; Spudich, 1990). A simple although blind way of taking these features into account is to consider nonlocal transitions between states with rate kernels $\omega_i(x, x', t - t')$, where x' is the location of the particle before excitation at time t' , x its location after the excitation at time t . These functions have to be l -periodic in both x and x' , and because of time translational invariance only $t - t'$ can describe temporal dependencies.

A simple illustration of the importance of nonlocality may be obtained in the following way (Ajdari *et al.*, 1993; Chauwin *et al.*, 1994). Consider a system consisting of two potentials $W_1(x)$ and $W_2(x)$ with coinciding minima and maxima, but with nonlocal transition rate kernels so that every transition from 1 to 2 is accompanied by a displacement d to the right, while every transition from 2 to 1 is accompanied by displacement to the left. Formally this reads $\bar{\omega}_i(x, x', t - t') = \omega_i(x') \delta(x - x' + (-1)^i d) \delta(t - t')$ for $i=1,2$. This system is equivalent to another one in which $W_2(x)$ is shifted with respect to $W_1(x)$ by a distance d , but in which the transition rates are local (see Fig. 7). In this simple picture, one clearly sees that macroscopic motion can result from a succession of downhill drifts. It is however essential to remember that, although surprising in view of Fig. 7, no current is generated if the transition rates obey detailed balance. The geometry (Fig. 7) in which progression to the right does not require actual hopping over potential hills is not less generic than the one depicted in Fig. 3. Consequently, in situations out of equilibrium, we now have a mechanism for motion without diffusive steps, so that the typical velocities and forces developed are fixed by

the slopes of the potentials: $v_{\text{typical}} \approx \mu \partial_x W \approx \mu W/a$. This allows an increase of force and velocity by a factor $W/k_B T$ as compared to our example of Fig. 6. This factor can be of order ten in biological systems and much more in artificial ones. Optimization is again reached by matching two pairs of time scales for a homogeneous perturbation and one pair for a localized one. Note, however, that partially localized excitations can now lead to monotonic $v(\Omega)$ with a maximum at $\Omega \rightarrow \infty$.

A qualitatively different illustration of the importance of time scales is obtained by choosing potentials that obey $W_2(x) = -W_1(x) + \text{const}$: permuting the lifetimes in states 1 and 2 exactly changes the sign of the velocity (Chauwin *et al.*, 1995). Note that the vanishing of the velocity for equal lifetimes is a consequence of the symmetry properties of the system and is not related to thermal equilibrium.

According to the arguments developed above, the two-state system can work in a continuum of different regimes of which only limiting cases have been described here. We have already shown that the absence of a velocity maximum as a function of the ATP concentration was in agreement with the idea of “active sites” used by biologists and expressed in our language by a highly localized transition rate $\omega_1(x)$. It would also be rewarding to extract information concerning the shapes of the potentials if possible. A two-level system may be a gross oversimplification of the biological complexity, but one would like for instance to be able to infer from the comparison between experiment and theory whether or not a diffusive step is taking place in the process. It turns out that, even though very beautiful experiments have been made on single motors (Svoboda *et al.*, 1993; Hunt *et al.*, 1994; Svoboda and Block, 1994), we are not able to answer this simple question. Indeed, within a wide range of potential shapes and parameter choices [including all the limits described in this paper provided $\omega_1(x)$ is highly localized] it is possible to reproduce (Chauwin, 1995) both the observed dependence of the velocity on the applied force or the ATP concentration and the stochastic “stepping” motion of the motor as reported by Svoboda *et al.* (1993). In the absence of independent knowledge of the mobilities and of the ATP hydrolysis rate, no answer to the above-stated question can be deduced with reasonable confidence.

This situation may change in the future, in particular if we can have access to efficiency measurements and to the force dependence of the velocity when the force helps the motors. Indeed, these two measures are sensitive to the existence of a “flat” state with constant W_2 . The efficiency depends very much on the probability for a motor to move over one period after one ATP hydrolysis event: in the shifted potential case it is very high, whereas if a diffusive step is needed it is significantly lower. Similarly, if an external force helps the natural motion, it is more effective and the resulting velocity is higher if one of the states is “flat” than if both of them exhibit significant “Kramers” barriers (Chauwin, 1995).

IV. COLLECTIVE EFFECTS

All the considerations developed up to now have been focused on the behavior of a single motor with one spatial degree of freedom and two “configurational” states. Molecular motors have been classified in two groups depending on whether they are designed to operate in groups (“rowers”) or individually (“porters”) (Leibler and Huse, 1991, 1993). In this section, we illustrate the original features that emerge when collections of motors rather than isolated ones are considered. Note that this case is relevant for experimental situations called “motility assays,” for muscle contraction and possibly for vesicle transport in cells. We show in particular that asymmetry of the potentials can become inessential in view of a possible symmetry-breaking transition (Jülicher and Prost, 1995). Other collective effects which result from steric hindrance between particles, are discussed by Derényi and Vicsek (1995) and Derényi and Ajdari (1996).

A natural generalization of the previous case for describing collective effects is obtained by attaching N particles at points $y_n = X + nq$, $n = 1 \dots N$, with equal spacing q to a rigid “backbone” while keeping the two-state model for each of them (Fig. 8). Here, X denotes the displacement of the backbone. In the following, we fo-

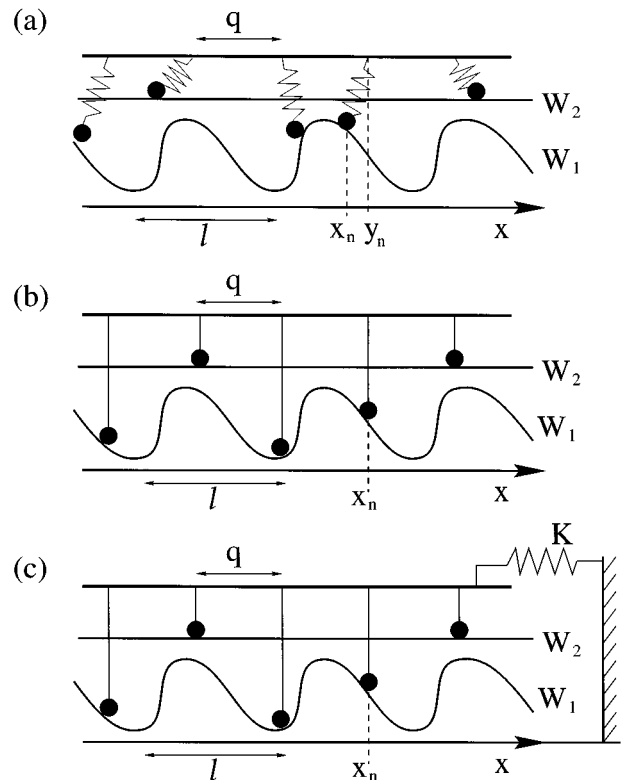


FIG. 8. (a) Schematic representation of a two-state many-motor system. Particles are attached periodically with spacing q via springs to a backbone at positions y_n . Particle positions are denoted by x_n . The potentials W_1 and W_2 are l -periodic. (b) Rigid coupling of particles with $y_n = x_n$. (c) Rigid system coupled elastically to the environment via an elastic element K .

cus on the case in which q/l is irrational and the periodicities of particle attachments and the potentials are incommensurate. This choice is motivated by the incommensurate arrangement of motors and filaments in muscle fibers. Indeed, muscle fibers are made of linear bundles of motors interacting with filaments, the respective periods of which are incommensurate. Similarly in motility assays, filaments are sedimented on a glass surface which is randomly coated with motors. Incommensurability or disorder allows particles to operate asynchronously, since different particles are at the same time in different states (H. E. Huxley, 1969).

In general, particles are attached to the backbone via elastic elements of elastic modulus c . The n th particle positioned at $x = x_n$ exerts a force $f_n = c(y_n - x_n)$ on the backbone. The rigidity of the backbone forces all particles to move with equal time-averaged velocity $v \equiv \dot{X} = \langle \dot{x}_n \rangle$. For an incommensurate system and large number N of particles, the force $f \equiv \sum_{n=1}^N f_n / N$ exerted per particle is given in the steady state by the time-averaged force of a single particle, $f = \langle f_n \rangle$.

Two extreme limits can be distinguished where the elastic elements are “soft” and “stiff,” respectively: For small $c \ll \bar{W} / l^2$, where \bar{W} denotes the maximal amplitude of the potentials, the particles are able to move many potential periods away from their attachment points: $|y_n - x_n| \gg l$. Since the particles in this case behave like free particles, the system behaves as if single-particle forces were simply added and no collective effects occur. For large $c \gg \bar{W} / l^2$, the behavior of the system changes significantly. In this case, $|x_n - y_n| \lesssim l$ and cooperative effects become important.

These cooperative effects can be discussed most easily for the case of a rigid coupling of particles to the backbone. This case, which is shown schematically in Fig. 8(b), corresponds to the limit of large c where $x_n = y_n$ and positional fluctuations of particles are neglected. The force exerted on the backbone by the n th particle is now given by $f_n = -\partial_x W_i(x_n)$. Since the potentials are periodic, the forces f_n depend only on the particle positions relative to the potential period. We therefore introduce a cyclic position variable $\xi \equiv x \bmod l$ with $0 \leq \xi < l$. The state of this rigid infinite system is characterized by the two p -periodic distribution functions $P_i(\xi)$ of a particle in the two states.

The incommensurability or disorder of particle attachments leads to a total distribution function $P(\xi) \equiv P_1(\xi) + P_2(\xi)$, which has constant value $P(\xi) = 1/l$ for large N . This results from the fact that for an incommensurate structure, each particle can be found at a different position ξ within the period l , and the interval $0 \leq \xi < l$ is homogeneously filled.

The equations of motion for the system read (Jülicher and Prost, 1995)

$$\begin{aligned} \partial_t P_1 + v \partial_\xi P_1 &= -\omega_1(\xi) P_1 + \omega_2(\xi) P_2, \\ \partial_t P_2 + v \partial_\xi P_2 &= \omega_1(\xi) P_1 - \omega_2(\xi) P_2. \end{aligned} \quad (19)$$

The excitation rates $\omega_1(\xi)$ and deexcitation rates $\omega_2(\xi)$ are those used in Eqs. (10) and (11). The velocity $v = \partial_t X$ is determined by

$$v = \mu(f_{\text{ext}} + f), \quad (20)$$

where μ is a mobility.³ The external force f_{ext} and the average force

$$f = - \int_0^l d\xi (P_1 \partial_\xi W_1(\xi) + P_2 \partial_\xi W_2(\xi)) \quad (21)$$

exerted by the potentials are normalized per particle. Equations of this type were discussed early by A. F. Huxley (1957) and Hill (1974). For an incommensurate system with $P_2 = 1/l - P_1$, the steady state obeys

$$v \partial_\xi P_1 = -(\omega_1(\xi) + \omega_2(\xi)) P_1 + \frac{\omega_2(\xi)}{l}, \quad (22)$$

$$f_{\text{ext}} = \frac{v}{\mu} + \int_0^l d\xi P_1 \partial_\xi (W_1 - W_2). \quad (23)$$

Equations (22) and (23) allow the determination of the external force $f_{\text{ext}}(v)$ that corresponds to a constant velocity v .

Equation (22) can be solved either analytically for some potential shapes or in a power expansion as a function of the velocity v :

$$P_1(\xi) = \sum_{n=0}^{\infty} P_1^{(n)}(\xi) v^n, \quad (24)$$

with

$$P_1^{(n)} = - \frac{1}{\omega_1 + \omega_2} \partial_\xi P_1^{(n-1)}, \quad (25)$$

and $P_1^{(0)} = \omega_2 / [(\omega_1 + \omega_2)l]$.

The force-velocity behavior can be written as

$$f_{\text{ext}} = f_\Omega^{(0)} + (\mu^{-1} + f_\Omega^{(1)})v + \sum_{n=2}^{\infty} f_\Omega^{(n)} v^n, \quad (26)$$

where

$$f_\Omega^{(n)} \equiv \int_0^l d\xi P_1^{(n)} \partial_\xi (W_1 - W_2). \quad (27)$$

Here, the index Ω denotes that all coefficients implicitly depend on the perturbation amplitude defined in Eq. (17). As in the single-motor case, one can easily check that the breaking of detailed balance is mandatory for obtaining any motion. For $\Omega = 0$, there is no spontaneous force, $f_\Omega^{(0)} = 0$, and $f_\Omega^{(1)}$ is always positive, which implies that thermal transitions of particles lead to additional dissipation, which increases friction (Tawada and Sekimoto, 1991; Leibler and Huse, 1993). $f_\Omega^{(0)}$ differs from zero only if both $\Omega \neq 0$ and the potentials are asymmetric. This coefficient $f_\Omega^{(0)}$ induces spontaneous motion

³Note that for simplicity we introduce a single coefficient μ independent of the state of the system, which describes the mobility of the complete system normalized per motor.

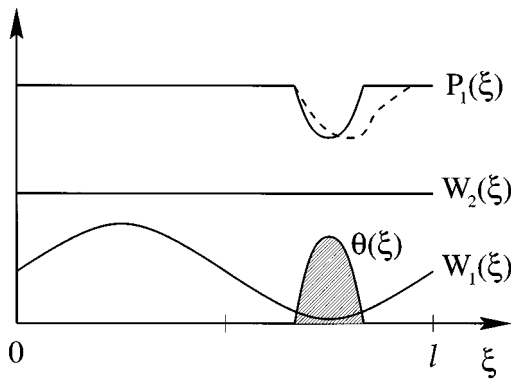


FIG. 9. Symmetric system with localized perturbation $\theta(\xi)$ and constant potential $W_2(\xi)$. The potentials are shown schematically together with the distribution $P_1(\xi)$ for $v=0$ within one potential period l . The broken line for P_1 indicates the deformation of P_1 for motion with $v>0$.

in asymmetric potentials, which corresponds to the mechanism for motion in the single-particle case.⁴

In order to discuss cooperative effects, we first consider a system with symmetric periodic potentials $W_i(\xi)$ and a symmetric localized perturbation $\theta(\xi)$. This situation is shown schematically in Fig. 9. Since the equations of motion depend only on $W_1 - W_2$, we have chosen W_2 to be constant. By symmetry, all even coefficients of the force expansion now vanish, $f_\Omega^{(0)} = f_\Omega^{(2)} = \dots = 0$, and $f_{\text{ext}}(v)$ is antisymmetric. If no external force is applied, the velocity obeys

$$0 = (\mu^{-1} + f_\Omega^{(1)})v + f_\Omega^{(3)}v^3 + O(v^5). \quad (28)$$

As long as $\mu^{-1} + f_\Omega^{(1)} > 0$, the only solution is $v=0$ and the system does not move. Broken detailed balance now allows $f_\Omega^{(1)}$ to become negative. At $\Omega = \Omega_c$ with

$$\mu^{-1} + f_{\Omega=\Omega_c}^{(1)} = 0, \quad (29)$$

a new situation occurs: For $\Omega > \Omega_c$ and $\mu^{-1} + f_\Omega^{(1)} < 0$, two moving solutions for $f_{\text{ext}}=0$ appear with

$$v_\pm = \pm \left(\frac{1}{f_\Omega^{(3)}} \frac{\partial f_{\Omega=\Omega_c}^{(1)}}{\partial \Omega} (\Omega - \Omega_c) \right)^{1/2}. \quad (30)$$

These two moving solutions are both stable while the nonmoving solution $v=0$ becomes unstable at Ω_c . The stability of steady states follows from the sign of the effective mobility $\mu_{\text{eff}}(v) \equiv (\partial f_{\text{ext}} / \partial v)^{-1}$. Therefore a continuous onset of motion occurs at $\Omega = \Omega_c$ via spontaneous symmetry breaking (see Fig. 10).

This spontaneous symmetry breaking can be understood qualitatively as follows. Consider an excitation perturbation $\theta(\xi)$ localized near the potential minimum

⁴This is not exactly true: The relation $P_1^{(0)} = 1/[1 + \exp[(W_1 - W_2)/T] + \Omega\theta(\xi)/\omega_2(\xi)l]$ implies that $f_\Omega^{(0)}$ is zero if $\theta(\xi)/\omega_2(\xi)$ is constant. Therefore, for constant ω_2 , no force is generated for a homogeneous perturbation $\theta(\xi) = 1/l$, which strongly differs from the single-particle behavior.

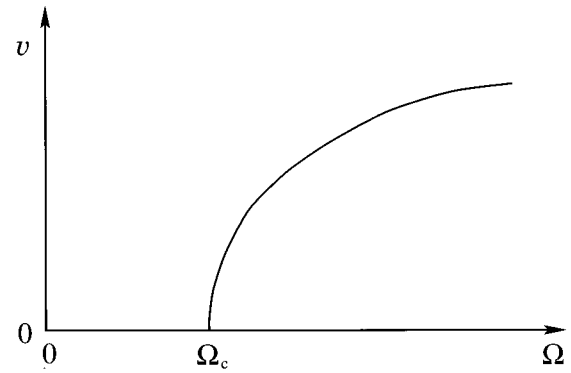


FIG. 10. Spontaneous velocity v as a function of the excitation amplitude for a symmetric system ($f_{\text{ext}}=0$). At the critical point $\Omega = \Omega_c$, spontaneous motion occurs continuously via spontaneous symmetry breaking.

as shown in Fig. 9. For simplicity, we neglect the effect of thermal transitions and assume that excitations occur only where $\theta(\xi) \neq 0$. Figure 9 shows the distribution $P_1(\xi)$ for $v=0$ as a solid line. Excitations $\Omega\theta(\xi)$ lead for $v=0$ to a depletion of $P_1(\xi)$ near the potential minimum. Since $\theta(\xi)$ and the potentials are symmetric functions, the force f vanishes. If the system is now perturbed and the backbone moves to the right with a small velocity v , the depletion of $P_1(\xi)$ is transported to the right as indicated in Fig. 9 by a broken line. Now, the population along the positive potential slope is depleted while the negative one has gained particles. As a result, the average force f pulls the backbone to the right and increases the initial fluctuation. This effect results in a negative value of $f_\Omega^{(1)}$. As the bare mobility μ stabilizes the nonmoving state, a critical excitation amplitude Ω_c has to be exceeded before instability is reached [see Eq. (29)].

This argument demonstrates that the localization of excitations near the potential minimum is important. If $\theta(\xi)$ were localized near the potential maximum, the depletion of the lower energy potential W_1 would have a stabilizing effect with $f_\Omega^{(1)} > 0$. Spontaneous motion would be suppressed.

The instability of the system can also be studied in the presence of an external force. Starting, for example, with $f_{\text{ext}}=0$ and $v=v_+$, the velocity decreases as a load $f_{\text{ext}} < 0$ is applied (see Fig. 11). As the minimum of the curve $f_{\text{ext}}(v)$ is reached, the steady state becomes unstable and a discontinuous change of the velocity occurs. Rather than moving against the force, the system now follows it. If the external force is reversed at this point, a similar instability occurs at the maximum of $f_{\text{ext}}(v)$.

The behavior of the symmetric system near $\Omega = \Omega_c$ is analogous to that of a ferromagnet near its critical point. The velocity v corresponds to the magnetization, the external force f_{ext} to the field, and Ω to the inverse temperature. Since each particle feels the mean force of all other particles, one finds the mean-field behavior $|v| \sim (\Omega - \Omega_c)^{1/2}$ as given by Eq. (30). Similarly, the velocity at $\Omega = \Omega_c$ obeys $v \sim f_{\text{ext}}^{1/3}$.

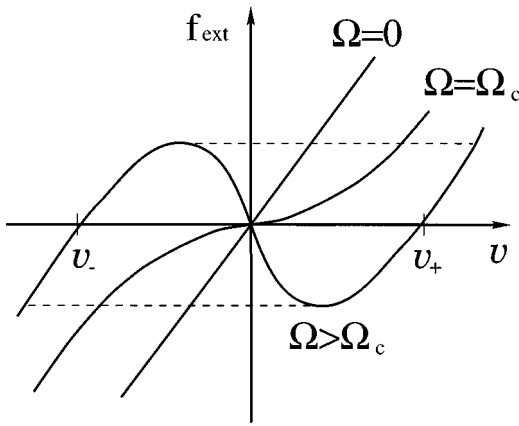


FIG. 11. External force f_{ext} as a function of velocity v for a symmetric system as defined in Fig. 9, for different values of the excitation amplitude Ω . At a critical value $\Omega = \Omega_c$, the solution $v = 0$ becomes unstable and two moving solutions with $v = v_{\pm}$ bifurcate for $f_{\text{ext}} = 0$.

Let us now consider asymmetric potentials. Symmetry breaking transitions are no longer possible since the velocity is nonzero at zero external force, for any nonvanishing excitation Ω . However, the possibility remains that a critical point may signal the appearance of velocity discontinuities as a function of the external force (see Fig. 12). At the critical excitation amplitude $\Omega = \Omega_c$, the corresponding curve $f_{\text{ext}}(v)$ exhibits a critical point for $f_{\text{ext}} = f_c$ and $v = v_c$ with diverging $\mu_{\text{eff}}(v_c) = \infty$. Beyond this critical point, a maximum and a minimum of $f_{\text{ext}}(v)$ occur, between which the corresponding steady states are unstable.

The resemblance of the curves shown in Fig. 12 with van der Waals isotherms suggests that the point (v_c, f_c, Ω_c) is equivalent to a liquid-gas critical point. From the expansion given in Eq. (26) one obtains the corresponding mean-field exponents $|v - v_c| \sim (\Omega$

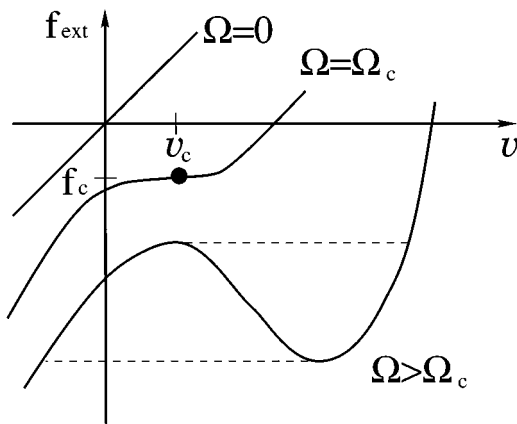


FIG. 12. External force f_{ext} as a function of velocity v for an asymmetric system, for different values of the excitation amplitude Ω . A critical point (f_c, v_c, Ω_c) exists. For $\Omega > \Omega_c$, the velocity shows instabilities and discontinuities as a function of the force f_{ext} .

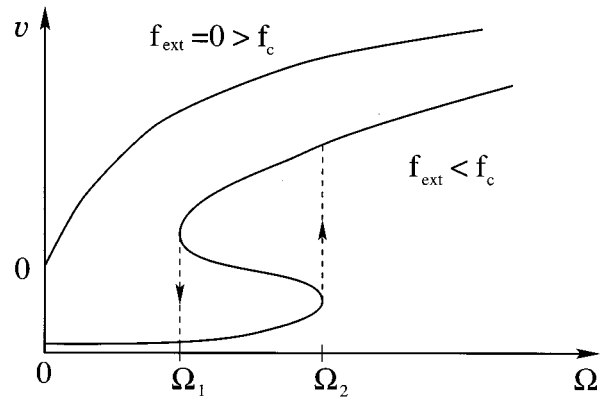


FIG. 13. Sliding velocity v of an asymmetric system as a function of the excitation amplitude Ω for two different external forces $f_{\text{ext}} > f_c$ and $f_{\text{ext}} < f_c$, where f_c denotes the critical force. For $f_{\text{ext}} < f_c$, discontinuities of v occur for $\Omega = \Omega_1$ and $\Omega = \Omega_2$.

$-\Omega_c)^{1/2}$ for $f_{\text{ext}} = f_c$ and $|v - v_c| \sim (f_{\text{ext}} - f_c)^{1/3}$ for $\Omega = \Omega_c$.

The dependence of the velocity on the excitation amplitude Ω is shown in Fig. 13 for two different values of the external force. If $f_{\text{ext}} > f_c$, no instability occurs and the velocity increases monotonically. For $f_{\text{ext}} < f_c$, discontinuities of the velocity occur: starting from the upper branch of the curve $v(\Omega)$ and decreasing Ω , the velocity exhibits a discontinuity at $\Omega = \Omega_1$, while, similarly, starting from the lower branch Ω and increasing, the velocity shows a discontinuity at $\Omega = \Omega_2$.

It is natural to wonder whether one would still have collective behavior of rigidly coupled particles if one made changes in the model. Indeed, for wide classes of potential functions and excitation localizations $\theta(x)$, collective behavior does exist. It also exists when motors are connected via springs to the rigid structure [see Fig. 8(a)]. Furthermore, fluctuations due to the finite length of the filaments may be shown to be unimportant in physiological cases when the number of motors is of the order of 100 (Jülicher and Prost, 1997).

Whereas such discontinuities of the sliding velocity as a function of external force may be difficult to find experimentally, some other consequences of this collective behavior may be more spectacular. Suppose that we connect the backbone to the filament externally via an elastic spring [see Fig. 8(c)]. This corresponds in a crude way to the structure found in striated muscles (Alberts *et al.*, 1994). Now, the effective external force is the actual external force plus the force due to the compression/dilation of the elastic spring: $f_{\text{ext}}^{\text{eff}} = f_{\text{ext}} - KX$ (where K is the spring constant and X the displacement of the spring extremity; note $v = dX/dt$). For $\Omega > \Omega_c$, and with a soft spring, the system will spontaneously start to oscillate in a characteristic way (Jülicher and Prost, 1997). This can be seen as follows: Taking for example the force-velocity relation shown in Fig. 11 of a symmetric system, starting with positive velocity, one finds that the spring is compressed more and more and the effective external force increases (in absolute value)

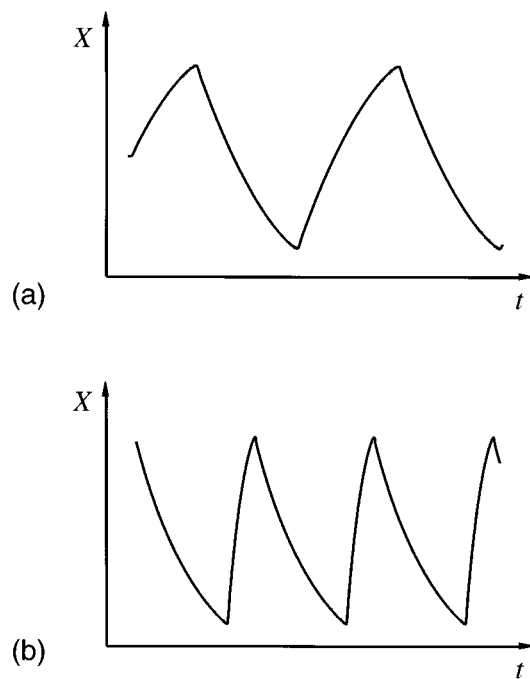


FIG. 14. Spontaneous oscillations of a collective system coupled via an elastic element to its environment. (a) The oscillations of a symmetric system show characteristic cusps at the maxima and minima where the sliding velocity changes discontinuously, corresponding to the instabilities in the force-velocity curve. (b) For an asymmetric system, the broken symmetry is reflected by the oscillation curve.

until the system reaches the lower unstable point of Fig. 11. At this point, the velocity changes sign discontinuously and the spring is now extended. This happens until the upper unstable point is reached and the velocity is again reversed discontinuously: As a result of the elastic coupling, the hysteresis loop of the first-order transition is transformed into an oscillation. See Fig. 14(a).

We described for convenience the example of a symmetric system, but oscillations persist for a wide range of asymmetric potentials. In fact, this asymmetry directly translates to the asymmetry of the oscillation curve as shown in Fig. 14. The conclusion of this analysis is that, in principle, muscle fibers could oscillate provided they are placed in appropriate conditions, even if they are not designed by nature to oscillate. Interestingly, skeletal muscle myofibrils have been shown to oscillate spontaneously *in vitro*, in the absence of any external driving (Yasuda *et al.*, 1996). The shape of the oscillations, the independence of their frequency and amplitude on any external load, and the frequency ranges are all consistent with this model. Spontaneous oscillations of asynchronous muscles, which operate in the wings of many insects such as wasps and bees, could also be related to this kind of collective behavior.

V. CONCLUDING REMARKS

The ideas that emerge from the analysis in the previous sections may be summarized fairly simply. Molecu-

lar motors, which are ubiquitous in eukaryotic life, are different from Carnot engines. A striking feature is that they are isothermal and therefore do not obey the Carnot efficiency rules. Thermal equilibrium (i.e., reversibility) is a singular limit: along some paths approaching equilibrium, the efficiency is strictly zero, while along some others it is constant. It is worth remarking that a departure from reversibility may lead to an increase in efficiency in contrast to what is sometimes assumed. This possibility is particularly clear in the collective motor case. In an almost symmetric system close to equilibrium, efficiency may be made as close to zero as one wishes, whereas beyond the spontaneous dynamical transition (i.e., moving away from reversibility), the efficiency easily reaches values as high as 50% to 60%.

The second lesson is that time scales play a very important role. For given interaction potentials, the efficiency of the operation of molecular motors depends on how lifetimes, drift times, and diffusion times are matched. Even the motor's direction of motion can depend on this matching. Note also that the comparison of our model's predictions for $v(\Omega)$ with experiments supports the idea of "active sites" developed earlier by biologists.

The third lesson is that motor collections might involve dynamic phase transitions, including hysteretic behavior and spontaneous oscillations. These phenomena are examples of mechano-chemical couplings involving thresholds. They might be prototypes of a larger class of "triggers" and "switches" in biology.

Eventually, the models described here may stimulate new types of experiments. Two-level systems made using artificial polar structures can easily be set up in practice and have been shown to induce motion of small objects in the absence of any global force or gradients, in agreement with theory. This can be done using very different technologies, both at microscopic scales (Leibler, 1994; Rousselet *et al.*, 1994; Faucheux *et al.*, 1995; Faucheux and Libchaber, 1995), and at more macroscopic ones (Osada *et al.*, 1992; Gorre *et al.*, 1996; Sandre and Silberzan, 1997). These systems not only allow one to study experimentally the effects described here but also may lead to new devices for the separation of particles (Ajdari and Prost, 1992; Ajdari *et al.*, 1993; Faucheux and Libchaber, 1995; Bier and Astumian, 1996).

ACKNOWLEDGMENTS

We are very grateful to S. Leibler and A. Maggs for introducing us to the problem of molecular motors. Special thanks are due to J. F. Chauwin, D. Mukamel, and L. Peliti for a particularly enjoyable collaboration. Interesting discussions with H. Braun, M. Bornens, P. G. de Gennes, I. Derenyi, J. Howard, L. Leibler, D. Louvard, G. Oster, A. Ott, D. Riveline, M. Siegert, J. Spudich, J. L. Viovy, and M. Wortis are also acknowledged. We thank L. Faucheux and A. Libchaber for sending us preprints of their work prior to publication. F.J. acknowledges support by NSERC of Canada.

REFERENCES

- Ajdari, A., 1992, Ph.D. thesis (Université de Paris 6).
- Ajdari, A., 1994, *J. Phys. I (Paris)* **4**, 1577.
- Ajdari, A., J. Lewiner, J. Prost, and J. L. Viovy, 1993, French patent 9311346.
- Ajdari, A., D. Mukamel, L. Peliti, and J. Prost, 1994, *J. Phys. I (Paris)* **4**, 1551.
- Ajdari, A., and J. Prost, 1992, *C. R. Acad. Sci. Paris II* **315**, 1635.
- Alberts, B., D. Bray, J. Lewis, M. Raff, K. Roberts, and J. D. Watson, 1994, *The Molecular Biology of the Cell* (Garland, New York).
- Astumian, R. D., 1997, *Science* **276**, 917.
- Astumian, R. D., and M. Bier, 1994, *Phys. Rev. Lett.*, **72**, 1766.
- Astumian, R. D., P. B. Chock, T. Y. Tsong, Y. Chen, and H. V. Westerhoff, 1987, *Proc. Natl. Acad. Sci. USA* **84**, 434.
- Bartussek, R., P. Hänggi, and J. G. Kissner, 1994, *Europhys. Lett.* **28**, 459.
- Bartussek, R., P. Reimann, and Hänggi, 1996, *Phys. Rev. Lett.* **76**, 1166.
- Bier, M., and R. D. Astumian, 1996, *Phys. Rev. Lett.* **76**, 4277.
- Büttiker, M., 1987, *Z. Phys. B* **68**, 161.
- Chauwin, J. F., 1995, Ph.D. thesis (Université de Paris 6).
- Chauwin, J. F., A. Ajdari, and J. Prost, 1994, *Europhys. Lett.* **27**, 421.
- Chauwin, J. F., A. Ajdari, and J. Prost, 1995, *Europhys. Lett.* **32**, 373.
- Chialvo, D. R., and M. M. Millonas, 1995, *Phys. Lett. A* **209**, 26.
- Derényi, I., and A. Ajdari, 1996, *Phys. Rev. E* **54**, 5-8 R.
- Derényi, I., and T. Vicsek, 1995, *Phys. Rev. Lett.* **75**, 374.
- Derényi, I., and T. Vicsek, 1996, *Proc. Natl. Acad. Sci. USA* **93**, 6775.
- Doering, C. R., 1995, *Nuovo Cimento* **17**, 685.
- Doering, C. R., W. Horsthemke, and J. Riordan, 1994, *Phys. Rev. Lett.* **72**, 2984.
- Duke, T., and S. Leibler, 1996, *Biophys. J.* **71**, 1235.
- Faucheux, L. P., L. S. Bourdieu, P. D. Kaplan, and A. J. Libchaber, 1995, *Phys. Rev. Lett.* **74**, 1504.
- Faucheux, L. P., and A. Libchaber, 1995, *J. Chem. Soc. Faraday Trans.* **91**, 3163.
- Feynman, R. P., R. B. Leighton, and M. Sands, 1966, *The Feynman Lectures on Physics* (Addison-Wesley, Reading, MA), Vol. I, Chap. 46.
- Finer, J. T., R. M. Simmons, and R. M. Spudich, 1994, *Nature (London)* **368**, 113.
- Gorre, L., E. Ioannidis, and P. Silberzan, 1996, *Europhys. Lett.* **33**, 267.
- Harada, Y., A. Noguchi, A. Kishino, and T. Yanagida, 1987, *Nature (London)* **326**, 805.
- Harms, T., and R. Lipowsky, 1997, unpublished.
- Hill, T. L., 1974, *Prog. Biophys. Mol. Biol.* **28**, 267.
- Hondou, T., and Y. Sawada, 1995, *Phys. Rev. Lett.* **75**, 3269.
- Hunt, A. J., F. Gittes, and J. Howard, 1994, *Biophys. J.* **67**, 766.
- Huxley, A. F., 1957, *Prog. Biophys.* **7**, 255.
- Huxley, A. F., and R. Niedegerke, 1954, *Nature (London)* **173**, 971.
- Huxley, A. F., and R. M. Simmons, 1971, *Nature (London)* **233**, 533.
- Huxley, H. E., 1969, *Science* **164**, 1365.
- Ishijima, A., T. Doi, K. Sakurada, and T. Yanagida, 1991, *Nature (London)* **352**, 301.
- Jülicher, F., A. Ajdari, and J. Prost, 1997, unpublished.
- Jülicher, F., and J. Prost, 1995, *Phys. Rev. Lett.* **75**, 2618.
- Jülicher, F., and J. Prost, 1997, *Phys. Rev. Lett.* **78**, 4510.
- Jung, P., J. G. Kissner, and P. Hänggi, *Phys. Rev. Lett.* **76**, 3436.
- Kedem, O., and S. R. Caplan, 1965, *Trans. Faraday Soc.* **61**, 1897.
- Kreis, T., and R. Vale, *Cytoskeletal and Motor Proteins*, 1993 (Oxford University Press, New York).
- Kron, S. J., and J. A. Spudich, 1986, *Proc. Natl. Acad. Sci. USA* **83**, 6272.
- Landauer, R., 1988, *J. Stat. Phys.* **53**, 233.
- Leibler, S., 1994, *Nature (London)* **370**, 412.
- Leibler, S., and D. Huse, 1991, *C. R. Acad. Sci. Paris III* **313**, 27.
- Leibler, S., and D. Huse, 1993, *J. Cell Biol.* **121**, 1357.
- Luczka, J., R. Bartussek, and P. Hänggi, 1995, *Europhys. Lett.* **31**, 431.
- Lymn, R. W., and E. W. Taylor, 1971, *Biochemistry* **10**, 4617.
- Magnasco, M. O., 1993, *Phys. Rev. Lett.* **71**, 1477.
- Magnasco, M. O., 1994, *Phys. Rev. Lett.* **72**, 2656.
- Mielke, A., 1995a, *Ann. Phys. (Leipzig)* **4**, 476.
- Mielke, A., 1995b, *Ann. Phys. (Leipzig)* **4**, 721.
- Millonas, M. M., 1995, *Phys. Rev. Lett.* **74**, 10.
- Millonas, M. M., and D. I. Dykman, 1994, *Phys. Lett. A* **183**, 65.
- Nishizaka, T., H. Myata, H. Yoshikawa, S. Ishiwata, and K. Kinoshita, 1995, *Nature (London)* **377**, 251.
- Osada, Y., H. Okuzaki, and H. Hori, 1992, *Nature (London)* **355**, 242.
- Peskin, C. S., G. B. Ermentrout, and G. F. Oster, 1994, in *Cell Mechanics and Cellular Engineering*, edited by V. Mow *et al.* (Springer, New York), p. xxx.
- Peskin, C. S., and G. F. Oster, 1995, *Biophys. J.* **68**, 202.
- Pringle, J. W. S., 1977, in *Insect Flight Muscle*, edited by R. T. Tregear (North-Holland, Amsterdam), p. 177.
- Prost, J., J. F. Chauwin, L. Peliti, and A. Ajdari, 1994, *Phys. Rev. Lett.* **72**, 2652.
- Rousselet, J., L. Salome, A. Ajdari, and J. Prost, 1994, *Nature (London)* **370**, 446.
- Sandre, O., and P. Silberzan, 1997, unpublished.
- Simon, S., C. Peskin, and G. Oster, 1992, *Proc. Natl. Acad. Sci. USA* **89**, 3770.
- Spudich, J. A., 1990, *Nature (London)* **348**, 284.
- Svoboda, K., and S. M. Block, 1994, *Cell* **77**, 773.
- Svoboda, K., C. F. Schmidt, B. J. Schnapp, and S. M. Block, 1993, *Nature (London)* **365**, 721.
- Tawada, K., and K. Sekimoto, 1991, *Biophys. J.* **59**, 343.
- Winkelmann, D. A., L. Bourdieu, A. Ott, F. Kinoshita, and A. Libchaber, 1995, *Biophys. J.* **68**, 2444.
- Yasuda, K., Y. Shindo, and S. Ishiwata, 1996, *Biophys. J.* **70**, 1823.
- Zhou, H. X., and Y. Chen, 1996, *Phys. Rev. Lett.* **77**, 194.